

Towards a Soft Pneumatic Glove for Hand Rehabilitation

Panagiotis Polygerinos, *Member, IEEE*, Stacey Lyne, Zheng Wang, *Member, IEEE*, Luis Fernando Nicolini, Bobak Mosadegh, George M. Whitesides and Conor J. Walsh*, *Member, IEEE*.

Abstract—This paper presents preliminary results for the design, development and evaluation of a hand rehabilitation glove fabricated using soft robotic technology. Soft actuators comprised of elastomeric materials with integrated channels that function as pneumatic networks (PneuNets), are designed and geometrically analyzed to produce bending motions that can safely conform with the human finger motion. Bending curvature and force response of these actuators are investigated using geometrical analysis and a finite element model (FEM) prior to fabrication. The fabrication procedure of the chosen actuator is described followed by a series of experiments that mechanically characterize the actuators. The experimental data is compared to results obtained from FEM simulations showing good agreement. Finally, an open-palm glove design and the integration of the actuators to it are described, followed by a qualitative evaluation study.

I. INTRODUCTION

Loss of the ability to move the fingers, whether partial or total, can greatly inhibit activities of daily living and can considerably reduce one's quality of life [1]. Physical therapy can be effective in regaining controlled hand movement for a variety of disabling conditions, such as physical injuries, diseases, overuse syndromes and neurological damages. Often rehabilitation for improving hand function requires the patient to perform repetitive task practice (RTP), which involves breaking a task down into individual movements and practicing these exercises to improve hand strength, accuracy, and range of motion [1], [2]. These methods, however, are labor intensive and costly due to the required long hours of training with a physical therapist [1]. A system where patients could carry out exercises on their own, either at home or in clinic, would make physical therapy more accessible and therefore would be beneficial for patients.

Manuscript received March 22, 2013. *Corresponding author.

Panagiotis Polygerinos, Zheng Wang, Luis Fernando Nicolini and Conor J. Walsh are with the Harvard Biodesign Laboratory, School of Engineering and Applied Sciences and Wyss Institute for Biologically Inspired Engineering at Harvard University, Harvard University Cambridge, MA, 02138, USA (e-mail: polygerinos@seas.harvard.edu; wang@seas.harvard.edu; walsh@seas.harvard.edu). Stacey Lyne is with the School of Engineering and Applied Sciences and Harvard College, Harvard University, Cambridge, MA, 02138, USA (e-mail: stacey.lyne@college.harvard.edu).

Bobak Mosadegh and George M. Whitesides are with the Department of Chemistry and Chemical Biology, Harvard University, 12 Oxford Street, Cambridge, MA 02138, USA, and Wyss Institute for Biologically Inspired Engineering, Harvard University, 60 Oxford Street, Cambridge, MA 02138, USA (e-mail: mosadegh@seas.harvard.edu; gwhitesides@gmwhgroup.harvard.edu).

Currently there is a wide variety of research groups that are developing robotic devices that can help in hand rehabilitation [2]-[6]. Studies indicate that stroke patients who have robotic assistance when performing intense repetitive movements can attribute this to significant improvement in hand motor functions [2], [3]. The main challenge associated with developing a hand rehabilitation device is that traditional robotic devices use actuators that are less compliant than the joints themselves [5]-[7]. These devices tend to be cumbersome and difficult to operate, mitigating the use of these devices by patients; particularly in a personal setting. To address these challenges, it has been proposed that the design of a soft wearable robotic device for hand rehabilitation could lead to greater advances for assistive or augmented activity in the home by providing safer human-robotic interactions and reducing cost [8].

One common way for actuating soft robots is with the use of fluidic McKibben actuators [9], [10]. For these actuators, a rubber tube surrounded by a braided shell provides a compliant, soft linear actuator. A related approach is being investigated by the Whitesides group [11] that employs soft pneumatic networks (PneuNets) embedded in elastomers which actuate (bend or curl) the material by air pressurization. Air is often preferred over fluid due to its low viscosity, compressibility, ease of storage, low weight, environmentally benign nature and that it can enable rapid actuation [11].

The option to integrate the above mentioned soft actuation methods into human rehabilitation devices are currently being investigated by an increasing number of research groups. Assistive devices are made utilizing the McKibben or, similar types of pneumatic muscle-like actuators [7], [12] and [13]. In addition, other developed rehabilitation devices use air chambers embedded in elastomers to perform bending motions required to assist in hand or finger exercises [14]-[16].

In this paper, a pneumatic rehabilitation glove is proposed that can achieve bending motions, similar to the flexing motion of human fingers. Soft elastomeric actuators based on the PneuNet technique are integrated into a neoprene glove to recreate the desired finger motions in a safe, cost affordable and compliant manner. The mechanical behavior of these actuators is geometrically analyzed and predicted using finite element modeling (FEM) methods. Their manufacturing procedure and mechanical characterization are also presented along with a comparison between experimental and theoretical data. Finally, the actuators are integrated into a soft material, open-palm glove configuration to demonstrate its ease of use and feasibility in performing a close fist.

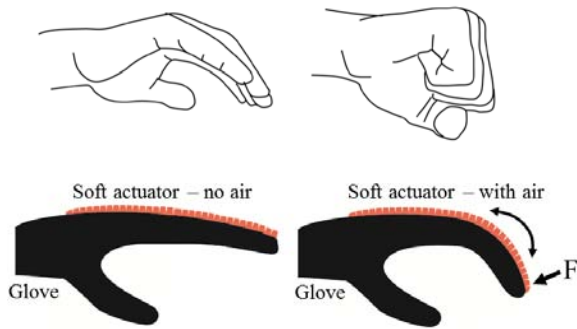


Fig. 1. Top: Characteristic rehabilitation exercise where the fingers go from an open state (left) to a closed state (right). Bottom: Conceptual function of the proposed soft robotic glove. Left: the soft actuator with no air pressure; fingers are in the open state. Right: the soft actuator with air pressure; fingers are assisted to move to the closed state.

II. DESIGN SPECIFICATIONS

One of the most common hand rehabilitation exercises aims in assisting a patient to gradually regain finger mobility and strength. For patients with surgically repaired fingers after traumatic injury, repetitive exercises are suggested that force the fingers to move from an open state into a closed one – there by moving the various finger joints through their range of motion (Fig. 1. - Top). However, patients are often incapable to perform these finger exercises correctly without having assistance from a physical therapist.

There are a number of design characteristics that need to be addressed in order to develop a wearable device that can successfully assist patients with hand rehabilitation exercises. The specific requirements for the soft glove are summarized in Table I and were obtained from discussions with physicians and a review of the medical literature. Firstly, the soft actuators performance should be such that bending curvatures can be achieved that can conform to the fingers in a closed fist configuration. The actuators should be then integrated in a wearable device (glove) in a manner that enables a patient with limited function to easily put it on and take it off. In addition, for safety reasons, the glove should be able to be quickly taken off the hand if needed. The typical variation across hand dimensions should be addressed either with a customizable glove design that fits to a specific user or with an adjustable one that fits some variation in size. Such a device should also be lightweight (<500g for the glove and actuators) so that gross patient motion is not restricted. Similarly, the overall profile should be kept as thin as possible so it does not provide resistance to finger motion if unpowered. Lastly, to be effective, actuation should be capable of at least 10 open-close finger cycles every minute.

To achieve the bending curvature of human fingers, soft pneumatic actuators were designed and attached on top of each finger in a glove configuration. Figure 1. - Bottom, illustrates the conceptual function of the proposed soft glove in which the fingers are assisted in bending when the actuators are pressurized. Compressed air was selected as the actuation source that provides the additional assistive force needed to allow patients to close their fist.

The glove size for this study was fixed to a No 7.5, i.e. a medium sized hand. All four fingers (pointer, middle, ring and small) use the same basic actuator design but with slightly

TABLE I
SPECIFICATIONS FOR A REHABILITATION SOFT GLOVE

Characteristics	Specifications
Weight	< 0.5 Kg
Profile	< 0.025 m
Glove Size	Customizable or adjustable
Degrees of Curvature	270° (similar to fingers)
Degrees of Freedom	3 (one for each finger joint)
Speed	Variable (up to 10 cycles/min)
Force at tip of actuator	Variable (patient dependent)
Safety	Easy to put on and take off Does not interfere with normal hand movement

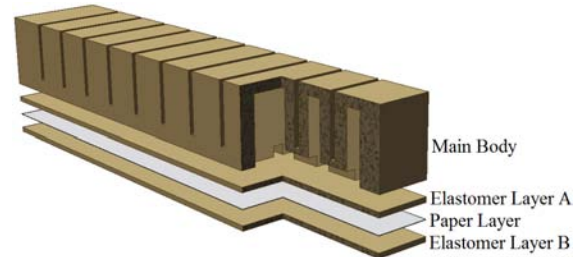


Fig. 2. Exploded view of the generic “PneuNets” soft actuator design. In cross section view: the PneuNets connected through the air channel.

different geometry to match the typical of each finger. The difference in actuator lengths is as follows: i) the pointer and ring finger actuators have the same length of 136 mm, ii) the middle finger actuator is 146 mm long and iii) the small finger actuator is 116 mm. It is noted that assisting thumb motion is not in the scope of this paper and therefore is omitted.

The bending actuators presented here are based on the PneuNet principle of operation [11]. The enclosed PneuNets run in parallel and along the entire length of the actuator. These actuators combine an extension with a strain limiting layer along their length. As they are pressurized internally, part of them grows while their strain limited portion does not. This causes the actuators to bend or even completely curl. Air flow between the PneuNets is achieved with an air channel located at the middle-bottom of the structure (Fig. 2.). For the inextensible component (paper), a density of 750 Kg/m³, a Young’s Modulus of 6.5 GPa and a Poisson’s ratio of 0.2 are defined. The mechanical properties for the paper layer are adopted from [17] and [18].

III. ACTUATOR DESIGN & CHARACTERIZATION

A. Actuator Geometrical Parameters

For the generic design of the actuators used in this study, a number of geometrical parameters can be identified (Fig. 3), as well as a larger number of their combinations, which could alter performance and behavior. In this work a specific subset of these parameters was explored (height of PneuNet, length, number of PneuNets and wall thickness) that are easy to vary experimentally.

In examining how actuator geometry affects its bending displacement and force capabilities, the overall length and width of actuator were kept constant as they were defined by the length and width of human fingers. Further, the total height (Fig. 3. – parameter *b*) of the actuator was constrained by the maximum acceptable glove profile (see Table I). Finally, the thickness of the bottom layers of the actuator were

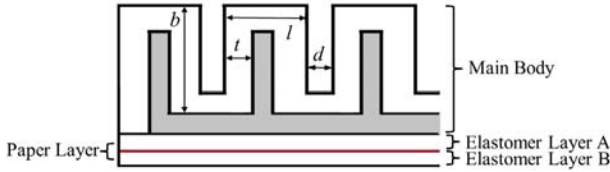


Fig. 3. Cross section of the soft actuator design showing: (l) number of PneuNets, (t) thickness of the walls, (b) height of PneuNets and (d) distance between PneuNets.

also constrained so as to limit the passive resistance to bending when unpressurized and eliminate the risk of rupture when pressurized. In this paper, three different parameters of the actuator were examined with the use of an analytical model for bending curvature and force performance that was validated using a FEM: i) number of PneuNets (Fig.4 – parameter l), ii) thickness of the walls (Fig.3. – parameter t) and iii) height of PneuNets (Fig.3. – parameter d).

B. Material Properties & Geometrical Analysis

Soft actuators/robots are typically made from hyperelastic materials such as silicone with non-linear behavior. When subjected to strain these materials have the ability to stretch several times more than their actual length and return to their initial shape. For this application, elastomeric samples (Elastosil M4601 A/B Silicone rubber RTV-2) with an elongation at break (strain) value of 700%, were tested according to ASTM D638 (Type IV) at a rate of 500 mm/min for tensile strength, and compression samples were compressed at a rate of 500 mm/min.

Due to the hyperelastic nature of the selected silicone, a second order hyperelastic mathematical model, Yeoh model [19], was used to fully describe the compression and extension phases of the material with coefficients $C_1=0.11$ and $C_2=0.02$. Compression and tensile data were plotted on a graph and fitted to the Yeoh hyperelastic material model in Matlab, see Fig. 4. As it can be observed from the data, the Yeoh model provides a good fit to the experimental data.

To provide a guideline for the actuator design of Fig. 2. and Fig. 3., a geometrical analysis was first carried out based on the hyperelastic Yeoh model. This analysis, although with simplifications and linearizations as discussed below, can provide insight into which geometrical parameters are most important to the bending and force exertion performances of the actuator.

Assuming incompressibility of the material across the width of the actuator, for each PneuNet the Yeoh model becomes of the form:

$$U = \sum_{i=1}^2 C_i \left(\lambda^2 + \frac{1}{\lambda^2} - 2 \right)^i, \quad (1)$$

Where $\lambda = \theta / \sin \theta$ is the principle stretch along the PneuNet, θ being the curve angle of the inflated PneuNet. Assuming the thickness of the PneuNet is much smaller than the air chamber height b , θ becomes a function of b and the inflation distance a :

$$\theta = \arcsin \left(\frac{4ab}{4a^2 + b^2} \right). \quad (2)$$

Hence stress $\sigma = \partial U / \partial \lambda$ is also a function of a and b :

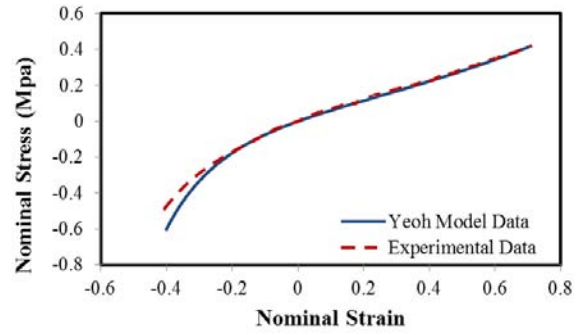


Fig. 4. Experimental and theoretical stress – strain curves of the hyperelastic silicone Elastosil M4601.

$$\sigma = \frac{\lambda^4 - 1}{\lambda^3} \left(2C_1 + 4C_2 \left(\lambda - \frac{1}{\lambda} \right)^2 \right). \quad (3)$$

Regarding each PneuNet as rigidly rotating around the interconnection point at the paper layer, the relationship between the supplied air pressure increase ΔP_i and the exerting force increase ΔF_E perpendicular to the PneuNet is:

$$\Delta F_E L_W = M_a \Delta P_i, \quad (4)$$

$$M_a = b^2 \left(2 - \frac{b^2}{b^2 - (2a - d)^2} \right), \quad (5)$$

where L_W is the width-justified lever of F_E . M_a determines how an increase in air pressure affects the exerted force at a certain configuration as a function of a . To achieve a larger M_a , a smaller a value is desirable. To reach the same curvature angle for a given actuator length, less expansion (smaller a) is required with a larger number of PneuNets. Since M_a is proportional to b^2 , having a larger b would result in a significant increase in M_a . On the other hand, the distance d between PneuNets should be kept small. Therefore, an actuator design which incorporates larger height, thinner walls and higher number of PneuNets is desirable.

C. Finite Elements Method (Abaqus CAE - FSI)

A FEM approach is described in this section that validates the geometrical parameters of section III-B and was used to predict the specific performance of final actuators designs. Through the FEM, the actuator design that offers best bending curvature and higher contact force at the tip of the actuator at lower pressure was investigated. The PneuNet actuators were treated with a standard/implicit FEM using the Abaqus 6.11 Computer Aided Engineering (CAE) package (Simulia, Dassault Systems). The elastomeric components of the actuator are categorized within the FE simulations as uniform – ‘solid’ elements, with the inextensible paper layer categorized as a ‘shell’. In all FE models the gravitational forces were taken into account and the air pressure was acting at all internal faces of the cavities (PneuNets).

During the FEM validation, different sets of parameters, including the number of PneuNets, the wall thickness and the height of PneuNets, were examined in a number of simulations. All other geometrical parameters were kept constant. To assess the bending curvature ability the nodes at one end of the actuator were constrained and then pressurized. The x and y displacements that occur can return the tip

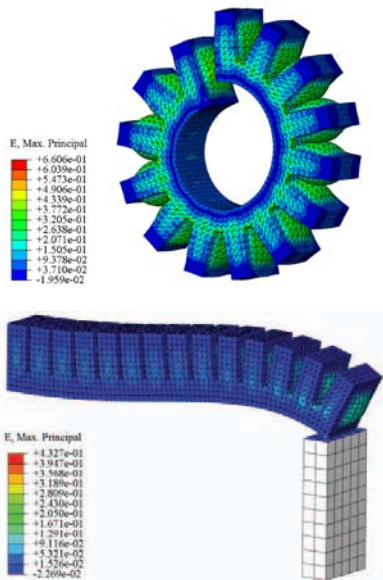


Fig 5. Top: Bending shape response for the FEM actuator. Bottom: Contact interaction shape response for the FEM model. The maximum strain is shown in the legends.

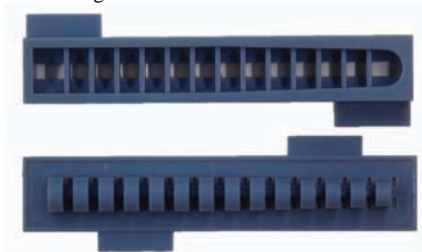


Fig. 6. The 3D printed two-parts mold of the middle finger soft actuator.

trajectory and thus the bending curvature. In the same way, the contact forces were assessed by bringing the actuator tip in contact with a solid rectangular block.

The results of the FEM simulations indicate that for a given geometry (based on the soft glove application) an actuator with 14 PneuNets, 1 mm wall thickness and 16 mm height PneuNets would meet the desired specifications. The selected parameter set fits the expectations of the analysis of section III-B. The bending shape response and shape of contact force response of the best performing simulated actuator design are shown in Fig. 5.

D. Manufacturing Process of Actuator

A two-part mold is created for the designed actuator using rapid prototyping techniques (3D printer – Connex 500, Objet). The two separate mold parts are shown in Fig. 6.

The casting of the actuators was made using an elastomer called Elastosil (described in section III – B). The two elastomeric parts (activator and silicone), while in liquid form, were mixed in a 9:1 ratio and poured inside the molds. A degassing procedure was required in which the molds were put in a vacuum and then in a pressure chamber. This procedure ensures that the casted elastomer will be free of trapped air bubbles that could potentially create failure points. Once degassed, the molds were put into an oven, at 70 C for 30 minutes, to accelerate the curing of the elastomer. A thin layer was also made of the same material that acts as the base component of the soft actuator and a rectangular piece of paper was embedded into it. This piece of paper, with a

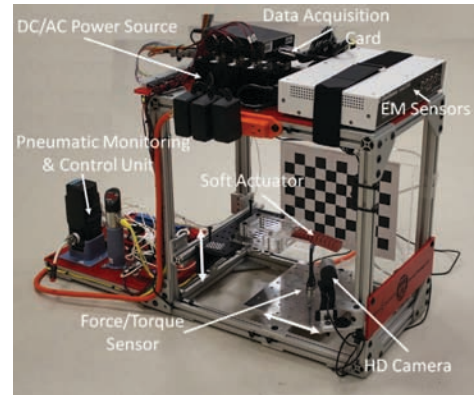


Fig. 7. Photograph of the developed soft actuators characterization platform showing all the individual hardware components.

thickness of 0.1 mm, acted as the inextensible layer of the actuator, restricting extension along its main axis. During the curing process the elastomer and paper were bonded together. On top of the paper layer, one last thin layer of liquid Elastosil was poured. The main body of the actuator is immersed deep enough to create a sealed connection with the bottom layers. Repeating the manufacturing steps, four actuators were manufactured, from which two of them, as described in section II, had the same length.

E. Experimental Results of Actuators

After selecting the best performing actuator design based on the FEM results, the four actuators (one for each finger of the human hand) were fabricated to characterize their ability to bend/curl and the force they can exert. It is noted that although four actuators were manufactured two of them (pointer and ring finger actuators) have the same dimensions thus, results were presented for three actuator sizes total.

To demonstrate the utility and accuracy of the simulations, an evaluation platform was developed that permits the simulated environments to be evaluated experimentally. This evaluation platform for soft actuators permits fast and easy characterization, incorporating multiple sensing modalities to obtain information on the intrinsic actuator performance. The platform (see Fig. 7.) contains pneumatic hardware (pressure/flow regulators and pressure/flow sensors, electro-pneumatic valves, relays and tubing), a multi-axis force sensor with signal conditioning unit and I/O digital/analogue data acquisition card to enable evaluation of control concepts, a temperature sensor in-line with the flow of the fluid and a high definition camera that overlooks the platform. In addition, the monitoring and control of the hardware components was achieved through a dedicated graphical user interface (GUI) written in LabView (LabView 2012, National Instruments).

The actuator ends were clamped in a rigid fixture, emulating the boundary constraints defined during the FEM simulations (see section III-C). A high definition camera (DSLR, Rebel T2i, Canon), utilizing a tripod, observed the actuator from the side so that the bending trajectory of its tip can be projected, i.e. camera was perpendicular to the actuator plane. The camera was registered and aligned using the aid of a printout of a checkerboard in the background of the actuator. This technique allowed lens distortion issues to be addressed and measurement accuracy to be enhanced. A metric ruler was also placed on the rigid fixture, next to the actuator, to provide

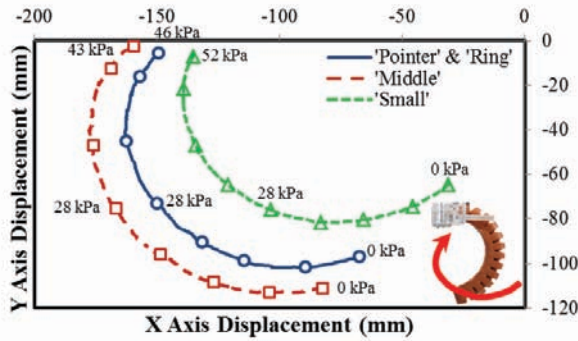


Fig. 8. Experimental tip displacement of all manufactured actuators. The actuators are horizontally aligned with the x axis and their free end starts bending in a clockwise fashion from point $(0, 0)$.

TABLE II

EXPERIMENTAL FORCE ESTIMATION FOR ALL ACTUATORS

Soft Actuator Identifier	Length (mm)	Force (Newtons) @ 43 kPa	Force Error (Newtons)
Pointer Finger Actuator	136	1.21	0.017
Middle Finger Actuator	146	1.09	0.014
Ring Finger Actuator	136	1.21	0.017
Small Finger Actuator	116	0.91	0.02

a correlation between number of pixels in the picture frames and the actual length.

To estimate the trajectory of the tip, the soft actuators were pressurized with air and depressurized three times while the camera captured the motion frames. For the post-processing of the frames a video analyzer software (Kinovea 0.8.15) was used. With this software the x and y coordinates of the actuator tip trajectory were tracked. The mean experimental results of the tip displacement for all the different actuator lengths were shown in Fig. 8. It is noted that due to gravity the actuators sag and thus pressurization coordinates start at lower points than $(0, 0)$. The maximum bending curvature observed was 320 degrees.

To calculate the force capacity a six axis force/torque sensor (Nano17, ATI Industrial Automation) was used to measure the magnitude of the resultant force generated. A short post was mounted on the force sensor and brought in contact with the tip of the actuator. The pressure inside the actuator was gradually increased, in increments of 6.89 kPa (1 psi), and the force exerted by its tip was recorded. The experiment was repeated three times to assess accuracy and repeatability. The mean force results for all actuators are shown in Table II.

To evaluate the validity of the FEM results, both the displacement trajectories and contact forces for the middle finger actuator were compared against the experimental results. Figure 9. demonstrates that the FE simulated tip trajectory and shape of the actuator were well in accordance with the results obtained from the physical actuator prototype with a maximum RMS error of 5.92%.

The differences in curvature results could be attributed to misalignments in the test set-up. An angular or translational misalignment between the placements of the back of the actuator with gravity will cause a different trajectory of the actuator. Additionally, misalignments in data recording devices (camera and video analyzer software) will affect the results. Another source of discrepancy may be from the FEM being inaccurate once extortions of the FE mesh become too large. In modeling the actuators, a simplified actuator design

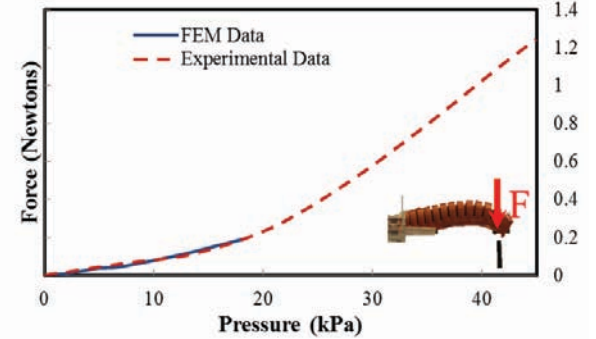
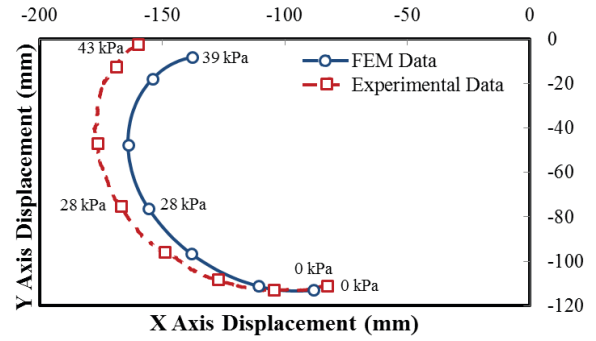


Fig. 9. Top: Comparison of FEM bending curvature and experimental data of the middle finger actuator. Bottom: Comparison of forces for FEM data and experimental data of the middle finger actuator.



Fig. 10. Top and bottom views of the prototype showing the soft actuators and the open palm glove configuration with the Velcro straps.

was used (without curved edges and tapering). This was done to aid the simulations in converging. However, some designs (usually the ones with the most deformation) would not converge to the maximum pressures, thus limiting the pressure at which results can be compared (e.g. Fig. 9 – Bottom). Future improvements of the FEM will require a re-meshing technique that applies new FE elements to the already deformed shape. Other general improvements that make the FEM model closer to reality may also need to be applied. Additionally, in the future, new design concepts for soft actuators will be explored that can achieve higher forces.

IV. GLOVE DESIGN & ACTUATOR INTEGRATION

The glove design proposed in this paper, Fig. 10., follows an open palm configuration to ensure quick, easy and safe fitting to the human hand. The main material used to manufacture the glove, an elastic fabric (neoprene) allows maximum conformability with fingers at all bending angles of the joints. All four soft actuators were mounted on the top surface of the glove, one above each finger, using thin Velcro



Fig. 11. Using the soft glove to grasp various objects.

straps. Small pockets were also fabricated that hug (surround) the fingers tips. These pockets, in combination with the straps, ensured that the glove can provide a soft but secure mount that can be easily dismantled from the human hand. The maximum profile of the glove did not exceed 2.5 cm and its total weight, including the actuators was around 160 grams.

The actuator design mimics the curving function of fingers. A smooth distribution of contact pressure over the entire length of the fingers minimizes concentrated pain effects and hence discomfort. The inextensible nature of the bottom layer of the actuator required an extensible material (elastic) be mounted along the back of the hand and connected to the end of the actuator. This was to address the extension of the finger length when going from a straight to curled configuration.

To evaluate the ability of the glove to provide assistance in the closing of fingers, several objects were brought in proximity and grasped with and without a participant wearing it. The objects examined for grasping vary in size and stiffness (an apple, a cup and a Styrofoam block). An increase in pressure inside the soft actuators resulted in a bending motion of the glove, forming a closed fist, and thus an external force to be applied on the objects. The internal pressures were measured to be 50 kPa, 45 kPa and 38 kPa for the apple, cup and foam respectively. The ability of the glove to conform around items through the control of its internal pressure and to exert forces (squeeze) is demonstrated in Fig.11.

V. CONCLUSIONS & FUTURE WORK

This paper reports the preliminary steps towards the development of a soft glove for hand rehabilitation. Pneumatic actuators based on the PneuNet architecture were geometrically analyzed and validated with FE model simulations. The selected geometrical designs resulting from the FEM were fabricated using a soft silicone material with high elongation characteristics.

Experimental results from tracking the tip of the actuators demonstrate their ability to curl more than 320 degrees and to provide forces high enough to assist passive human fingers in closing i.e. impaired fingers that have some or no stiffness. The FEM results are also compared with the experimental data demonstrating that the proposed model can be used to predict the overall behavior of soft actuators based on the PneuNet architecture. Lastly, a soft and easy method to fit the actuators on a human hand is presented along with preliminary experiments that demonstrate the feasibility of the glove.

Future steps involve improvement of the FEM's to accommodate a wider range of actuator geometries and sizes. Further, other approaches to manufacture such actuators could potentially increase the amount of pressure they are able to

withstand and thus be able to deliver higher forces. Finally, methods for the evaluation of the mechanical performance of the entire glove and trials with hand impaired participants will be pursued.

ACKNOWLEDGMENT

The authors would like to thank Prof. Katia Bertoldi, Dr. Jongmin Shim and Mr. Bas Overvelde, from the Bertoldi Group for mechanics of materials and structures at Harvard University for their help with the finite element modeling of the soft actuators.

REFERENCES

- [1] C. D. Takahashi, L. Der-Yeghiaian, V. Le, R. R. Motiwala, and S. C. Cramer, "Robot-based hand motor therapy after stroke", *Brain*, vol. 131, pp. 425-437, 2008.
- [2] S. Ueki, Y. Nishimoto, M. Abe, H. Kawasaki, S. Ito, Y. Ishigure, J. Mizumoto, and T. Ojika, "Development of virtual reality exercise of hand motion assist robot for rehabilitation therapy by patient self-motion control", in *Proc. IEEE Int. Conf. Eng. Med. Biol. Soc.*, 2008, pp. 4282-4285.
- [3] N. G. Kutner, R. Zhang, A. J. Butler, S. L. Wolf, and J. L. Alberts, "Quality-of-life change associated with robotic-assisted therapy to improve hand motor function in patients with subacute stroke: a randomized clinical trial", *Physical therapy*, vol. 90, pp. 493-504, 2010.
- [4] A. Polotto, F. Flumian, Z. G. Xiao, P. Boscariol, and C. Menon, "Index finger rehabilitation/assistive device", in *Proc. IEEE Int. Conf. Engineering in Medicine and Biology Society*, 2012, pp. 1518-1523.
- [5] E. Carmeli, S. Peleg, G. Bartur, E. Elbo, and J. J. Vantine, "HandTutor™ enhanced hand rehabilitation after stroke-a pilot study", *Physiotherapy Research International*, vol. 16, pp. 191-200, 2011.
- [6] Gloreha. (2012), "The HAnd REhabilitation GLOve", available: <http://www.gloreha.it/index.php?lang=en>.
- [7] L. Connelly, M. E. Stoykov, Y. Jia, M. L. Toro, R. V. Kenyon, and D. Kamper, "Use of a pneumatic glove for hand rehabilitation following stroke", in *Proc. IEEE Int. Conf. Engineering in Medicine and Biology Society*, 2009, pp. 2434-2437.
- [8] N. Tsagarakis and D. G. Caldwell, "Improved modelling and assessment of pneumatic muscle actuators", in *Proc. IEEE Int. Conf. Robot. Autom.*, 2000, pp. 3641-3646.
- [9] G. K. Klute, J. M. Czerniecki, and B. Hannaford, "McKibben artificial muscles: pneumatic actuators with biomechanical intelligence", in *Proc. IEEE/ASME Int. Conf. Advanced Intelligent Mechatronics*, 1999, pp. 221-226.
- [10] A. M. Bertetto and M. Ruggiu, "Characterization and modeling of air muscles", *Mech Res Commun*, vol. 31, no. 2, pp. 185-194, 2004.
- [11] F. Iliovski, A. D. Mazzeo, R. F. Shepherd, X. Chen, and G. M. Whitesides, "Soft robotics for chemists", *Angewandte Chemie*, vol. 123, pp. 1930-1935, 2011.
- [12] D. Sasaki, T. Noritsugu, M. Takaiwa, and H. Yamamoto, "Wearable power assist device for hand grasping using pneumatic artificial rubber muscle", in *Proc. IEEE Int. Workshop ROMAN*, 2004, pp. 655-660.
- [13] E. Koeneman, R. Schultz, S. Wolf, D. Herring, and J. Koeneman, "A pneumatic muscle hand therapy device", in *Proc. IEEE Int. Conf. Engineering in Medicine and Biology Society*, 2004, pp. 2711-2713.
- [14] S. Wakimoto, K. Ogura, K. Suzumori and Y. Nishioka, "Miniature soft hand with curling rubber pneumatic actuators", in *Proc. IEEE Int. Conf. Robot. Autom.*, Kobe, Japan, 2009, pp. 556-561.
- [15] D. Mingcong, W. Aihui, S. Wakimoto and T. Kawashima, "Characteristic analysis and modeling of a miniature pneumatic curling rubber actuator", in *Proc. IEEE Int. Conf. Advanced Mechatronic Systems*, 2011, pp. 534-539.
- [16] A. A. M. Faudzi, M. R. M. Razif, I. N. A. M. Nordin, K. Suzumori, S. Wakimoto and D. Hirooka, "Development of bending soft actuator with different braided angles," in *Proc. IEEE/ASME Int. Conf. Advanced Intelligent Mechatronics*, 2012, pp. 1093-1098.
- [17] J. Castro and M. Ostoja-Starzewski, "Elasto-plasticity of paper", *International Journal of Plasticity*, vol. 19, no. 12, pp. 2083-2098, 2003.
- [18] T. Yokoyama, K. Nakai, "Evaluation of in-plane orthotropic elastic constants of paper and paperboard", *Annual Conference & Exposition on Experimental and Applied Mechanics*, 2007.
- [19] O. H. Yeoh, "Some forms of the strain energy function for rubber", *Rubber chemistry and technology*, vol. 66, no. 5, pp. 754-771, 1993.